Journal of Energy Technology

STATIC MODEL OF TEMPERATURE DISTRIBUTION IN A PHOTOVOLTAIC MODULE

STATIČNI MODEL TEMPERATURNE PORAZDELITVE V FOTONAPETOSTNEM MODULU

Klemen Sredenšek[1ℛ], Sebastijan Seme[1,2], Gorazd Hren[1]

Abstract

The primary objective of this paper is to present a static model for calculating the temperature distribution in a photovoltaic module using the finite element method. The paper presents in more detail the theoretical background of solar radiation, heat transfer, and the finite element method. The results of the static model are evaluated using temperature measurements of a photovoltaic model, which were performed at the Institute of Energy Technology, Faculty of Energy Technology, University of Maribor. The results of the regression analysis show a good concurrence between the measured and modelled values of the temperature of the photovoltaic module, especially on days with a higher share of the direct component of solar radiation.

Povzetek

Glavni cilj tega prispevka je predstavitev statičnega modela za izračun temperaturne porazdelitve v fotonapetostnem modulu po metodi končnih elementov. V prispevku je podrobneje predstavljeno teoretično ozadje sončnega sevanja, prenosa toplote in metode končnih elementov.

ℛ, Corresponding author: Klemen Sredenšek, M.Sc., E-mail address: klemen.sredensek@um.si

[1] University of Maribor, Faculty of Energy Technology, Hočevarjev trg 1, 8270 Krško, Slovenia

[2] University of Maribor, Faculty of Electrical Engineering and Computer Science, Koroška cesta 46, 2000 Maribor, Slovenia

Rezultati statičnega modela so ovrednoteni z meritvami temperature fotonapetostnega modela, ki so bile izvedene na Inštitutu za energetiko (Fakulteta za energetiko Univerze v Mariboru). Rezultati regresijske analize med izmerjenimi in izračunanimi vrednostmi temperature fotonapetostnega modula prikazujejo dobro ujemanje predvsem v dnevih z večjim deležem neposredne komponente sončnega sevanja.

1   INTRODUCTION

The efficiency of converting solar energy into electricity of today's photovoltaic (PV) modules ranges between 14-21 %, which means that about 80% of the solar radiation that reaches the surface of PV modules is converted into heat losses or reflected into the environment. In addition to the aforementioned, the efficiency of converting solar energy into electricity depends mainly on materials, optical losses, and other meteorological parameters. As a result, raising the temperature of a PV module significantly reduces its efficiency [1]. To this end, researchers began to develop various cooling systems that would lower the temperature of PV modules and consequently increase their efficiency [2-4]. In order to calculate the temperature of a PV module, various static mathematical models have been developed, which accurately determine the temperature of a PV module by means of correlations between heat transfer mechanisms and meteorological parameters. The simplest and most commercially used way to calculate the temperature distribution in a PV module is the Nominal Operating Cell Temperature (NOCT) model. In addition to the solar radiation and ambient temperature, all other parameters are normalised to the standard test conditions (STC) of the PV module specified by the manufacturer of the PV module. In addition to the NOCT model, a model called SNL or Sandia (Sandia National Laboratories) is also used to calculate the temperature distribution in the PV module with additional consideration of the wind speed. Due to the simplified use, the results of both models can deviate by up to 20 °C compared to the measurements of the operating temperature of PV modules [5]. In general, most of the aforementioned models are based on a state of dynamic equilibrium, which assumes that the temperature of PV modules responds instantly to atmospheric conditions. However, the conditions in the atmosphere are very dynamic and change rapidly. On this basis, dynamic models with concentrated parameters were developed [6,7], which represent greater accuracy while addressing the uniform temperature distribution through the layers of PV modules. In addition to the aforementioned dynamic models, static models with concentrated parameters [8] or numerical models (discrete methods) can also be used for accurate calculation. As mentioned above, the optical losses and electricity production of PV modules must also be considered in order to obtain an accurate calculation. In their research, specific authors [9-13] developed so-called dynamic and static thermo-electric models, which determine the operating temperature of PV modules and the production of electricity. However, it is necessary to provide enough accurate measurements to respond to a dynamic or static model [13]. For this purpose, measurement data from the year of installation of the measuring equipment were used to reduce the error between the measured and modelled results.

This paper consists of four sections. The first section provides an introduction to the research topic. The second section describes the methodology of solar radiation, heat transfer, and the finite element method, while the third section presents the results of the static model and the validation with measurements. The fourth and final section discusses the conclusions of the paper.

2   MATERIALS AND METHODS

2.1   Solar radiation

The electromagnetic waves of the Sun's rays present the power density of solar radiation that the Earth receives per unit area. Solar radiation is basically divided into direct radiation, diffuse radiation of the sky (scattered radiation), and reflected radiation (radiation reflecting off the surroundings and falling on the observed surface). In the conversion of solar energy into electrical or thermal energy, the most important contribution is direct radiation and, to a lesser extent, the contribution of diffuse and reflected radiation. To correctly determine the solar radiation on the observed surface (at a specific inclination and orientation angle), it is necessary to take into account the geometric relations between the Sun and the Earth, such as latitude (L), longitude (l), declination angles (δ), hourly angle of the Sun (ω), zenith angle (z), solar altitude angle (α_s), the azimuth angle of the Sun (γ_s), inclination angle (β), orientation angle (γ) and angle of incidence of the Sun's rays (i). Using the aforementioned parameters and some specific models [14-16], solar radiation can be predicted for any inclination and orientation angle, given by (2.1).

$$G_t(t) = G_b(t) \cdot \left(\frac{\cos(i(t))}{\sin(\alpha_s)} \right) + G_d(t) \cdot \left(\frac{1 + \cos(\beta(t))}{2} \right) + G_h(t) \cdot \left(\frac{(1 - \cos(\beta(t)) \cdot \rho_r)}{2} \right) \qquad (2.1)$$

$G_t(t)$, $G_b(t)$, $G_d(t)$, and $G_h(t)$ are total, direct, diffuse, and global solar radiation, while the reflection factor ρ_r varies from 0 to 1, depending on the different types of surface substrates.

2.2   Heat transfer

Heat transfer deals with all the processes in which energy is transferred due to temperature differences between bodies or in matter. Heat transfer plays a vital role in many technological processes, such as accelerating heat transfer in heating or limiting heat transfer in cooling. Heat transfer can basically be divided into three mechanisms: conduction, convection, and radiation [17].

Conduction is the diffuse transport of thermal energy, in which the constituent particles of matter (atoms, molecules, electrons, and ions) rotate, vibrate, and move in a straight line. The corresponding kinetic energy increases with increasing temperature, with the kinetic energy being transferred from the higher temperature to the lower temperature range. The conduction in the case of the PV module is due to the thermal gradients between the different layers of the PV module. Fourier established a connection called the Fourier Law for one-dimensional heat transfer, which is given by (2.2), where λ is the thermal conductivity of the material.

$$q = -\lambda \frac{dT}{dx} \quad \text{oz.} \quad q(x) = -\lambda \nabla T(x) \qquad (2.2)$$

The negative sign in (2) tells us that heat is transferred from the area with the higher temperature to the area with the lower temperature [17].

Convection presents a mechanism of heat transfer through the movement of a liquid or gas. In the event that the original stationary liquid is in contact with a warmer surface, its density decreases and begins to rise due to buoyancy. Such a phenomenon is called natural convection, given by (2.3), where A is the wall surface area, T_s is the wall temperature, T_f is the fluid temperature, and δ is the boundary layer thickness.

$$\phi = \lambda\, A\, \frac{T_s - T_f}{\delta} \tag{2.3}$$

Given that the wall thickness cannot be measured separately from the thermal conductivity λ, the convective heat transfer coefficient α was introduced, where the basic convection equation is given by (2.4) [17].

$$q = \alpha\left(T_s - T_f\right) \tag{2.4}$$

The convective heat transfer coefficient α was first proposed for vertical surfaces (0.5 x 0.5m) in 1924 and is still the most used equation today, involving liquid/gas velocity (given by (2.5)).

$$\alpha = 5.7 + 3.8\, v \tag{2.5}$$

Heat transfer by **radiation** differs from conductive and convective heat transfer, firstly due to the possibility of transfer through empty space and secondly due to the transfer of the proportionality of heat to the fourth exponent. The primary connection for the radiant heat flux from an optically grey surface is Stefan-Boltzmann's Law given by (2.6), where T is the body surface temperature, ε is the emissivity of the body surface, and σ is the Stefan-Boltzmann constant.

$$q = \sigma\, \varepsilon\, T^4 \tag{2.6}$$

2.3 Fourier partial differential equation for steady-state heat transfer

In the previous subsection, three basic heat transfer mechanisms were presented, which allow the heat flux to be determined at each point. For this reason, a partial differential equation (PDE) is given, representing the internal body temperature. Imagine a small cube of volume $dV = dx\, dy\, dz$, presented as part of a three-dimensional body in Figure 1. Under the influence of the temperature distribution $T(x)$ inside the body, heat flows q_k and q_{k+dk} ($k = x, y, z$) occur through six surfaces of the cube. Using the first-order Taylor approximation given in (2.7), the following heat transfer equations of the cube can be expressed from (2.8) to (2.10).
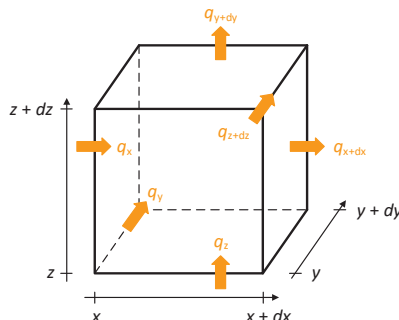
Figure 1: A cube with volume dV and heat flows through surfaces.

$$q_{k+dk} = q_k + \frac{\partial q_k}{\partial k} dk \quad (k = x, y, z) \tag{2.7}$$

$$\text{along the } x\text{-}axis: \left(q_x - q_{x+dx} \right) dydz = -\left(\frac{\partial q_x}{\partial x} \right) dxdydz = -\left(\frac{\partial q_x}{\partial x} \right) dV \tag{2.8}$$

$$\text{along the } y\text{-}axis: \left(q_y - q_{y+dy} \right) dxdz = -\left(\frac{\partial q_y}{\partial y} \right) dydxdz = -\left(\frac{\partial q_y}{\partial y} \right) dV \tag{2.9}$$

$$\text{along the } z\text{-}axis: \left(q_z - q_{z+dz} \right) dxdy = -\left(\frac{\partial q_z}{\partial z} \right) dzdxdy = -\left(\frac{\partial q_z}{\partial z} \right) dV \tag{2.10}$$

2.4 Finite element method

The finite element method (FEM) is used to predict mechanical, thermal, and electromagnetic systems. The FEM analysis consists of domain discretisation into finite elements, formulation of system equations, and graphical presentation. Based on the PDE given by (2.7), the boundary conditions can be determined, classified into three groups in heat transfer: Dirichlet, Neumann, and Cauchy boundary conditions.

Dirichlet boundary conditions (first type) are given by (2.11) and determine the temperature T_s at the domain/body boundary:

$$T(x,t) = T_s(x,t) \tag{2.11}$$

Neumann boundary conditions (second type) are given by (2.12) and determine the partial temperature discharge according to Fourier's Law concerning the vector n in the event of heat flux q_s from the domain/body (perpendicular to the body) [18].

$$q_s(x,t) = -\lambda \frac{\partial T}{\partial n}(x,t) \implies \frac{\partial T}{\partial n}(x,t) = -\frac{q_s(x,t)}{\lambda} \tag{2.12}$$

Cauchy boundary conditions (third type): A thermal iteration occurs between the body and the T_f fluid (shown in Figure 2). To quantify this, the body's boundaries represent the 'control volume' for an energy balance. As the thickness of the boundaries is zero, no energy can be stored within, which means that all the heat that enters the body (via conduction) must also leave the body (via convection). Cauchy boundary conditions are given by (2.13):

$$-\lambda \frac{\partial T}{\partial n}(x,t) = \alpha \left(T(x,t) - T_f \right) \tag{2.13}$$

3 RESULTS AND DISCUSSION

This section is divided into three subsections. The first subsection describes the experimental set-up of dual-axis PV tracking systems and measurement equipment, while the second

describes the model set-up performed in Ansys Transient Thermal software. The last subsection covers the validation of the model with measurements.

3.1 Experimental set-up

The input parameters of the static thermal model are various measurements performed in the experimental field of dual-axis PV tracking systems set at the Institute of Energy Technology, Faculty of Energy Technology, University of Maribor. In addition to the basic components of the PV system, dual-axis PV tracking systems also consist of several measuring devices, such as pyranometers, anemometers, and sensors for measuring the ambient temperature and the temperature of the PV module (in the center of the PV module), shown in figure 2. The PV system consists of 20 PV modules from the manufacturer PV Future with a nominal power of 260 W_p, and a total installed power of 5.2 kW_p [19]. The sampling time of the measurements is 30 min.
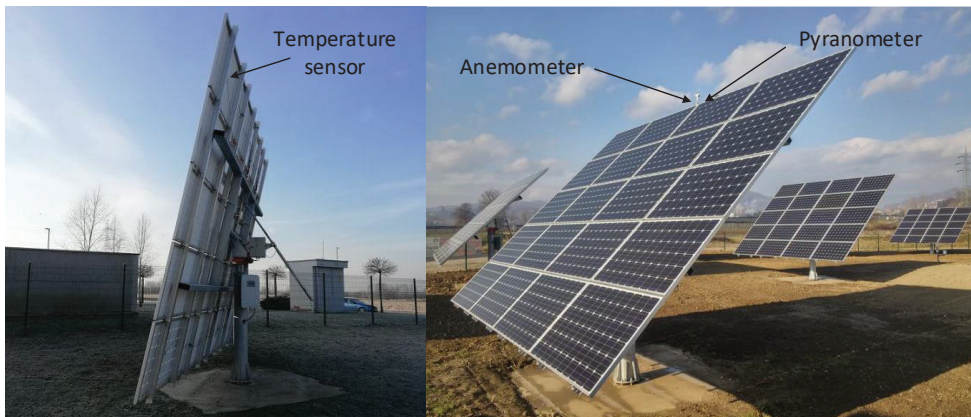
Figure 2: Experimental set-up: Dual-axis PV tracking system equipped with measuring devices.

3.2 Model set-up

The aim of the model is to analyse the temperature distribution on the rear of the PV module. Therefore, the model set-up performed in the Ansys Transient Thermal software is presented in detail below. A non-stationary analysis (depending on time) of heat transfer through the PV module was performed based on ambient temperature and wind speed measurements. The 3D model of the PV module was created in the Solidworks software package and imported into the Ansys Workbench software package. This was followed by determining the properties of the materials and discretising the model or dividing the geometry of the model into a finite number of small elements. Considering that the observed point was on the rear of the PV module, or more precisely at the location of the temperature measuring sensor, the model was simplified due to the calculation speed (removing the PV module's aluminum frame). The model grid was

automatically generated due to the simple geometry, using hexahedral elements as shown in Figure 3. The mesh of the model consists of 5,250 elements and 38,440 nodes.
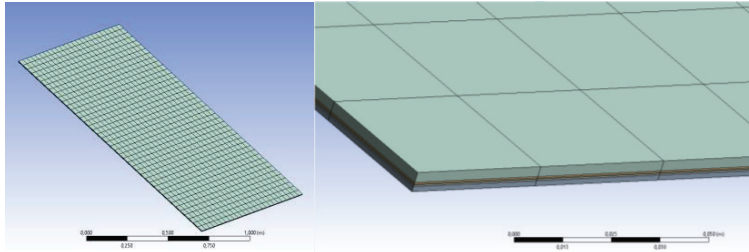
Figure 3: *Discretisation of the model.*

The PV module consists of protective glass, EVA foil, PV cells (monocrystalline silicon), EVA foil, and PolyVinyl Fluoride foil (PVF - Tedlar), as shown in Figure 4. The properties of the described materials were determined as constant values since temperatures of the PV module do not drastically affect the changes in the parameters. The thermal parameters of the materials used in the considered PV module are shown in Table 1.
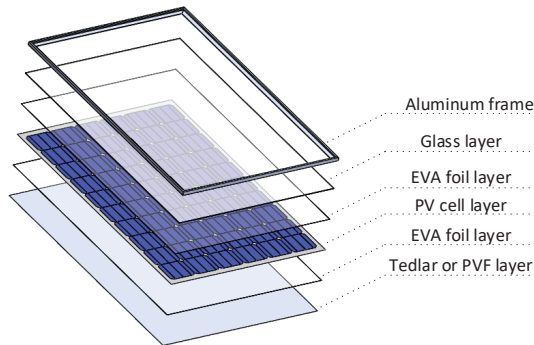
Figure 4: *Composition of the PV module by layers.*

Table 1: *Thermal parameters of the materials used in the PV module (based on the literature [9,11,13])*

	C [J/kgK]	*k* [W/mK]	*d* [mm]	*ρ* [kg/m³]
Glass	500	1.8	4	3000
EVA foil	2090	0.35	0.4	960
PV cell	677	148	0.3	2330
PVF foil	1250	0.2	0.4	1200

The boundary conditions applicable to heat transfer were subsequently defined for the PV module. As described in subsections 2.2 and 2.4, heat transfer is divided into three mechanisms: convection, conduction, and radiation. The first boundary condition involved determining the direction and magnitude of heat flux to the surface of the PV module (glass), while the second boundary condition included all other surfaces of the PV module that are subject to ambient temperature and velocity and wind direction to the surface. The determination of the boundary conditions for convection and heat flux is shown in Figure 5.

a)   b)
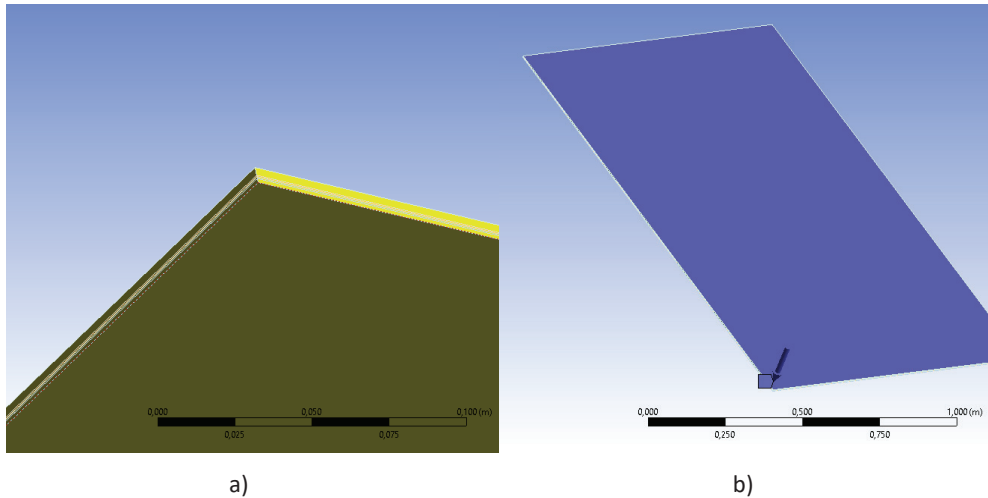
Figure 5: *Determination of the boundary conditions – a) convection and b) heat flux.*

3.3   Validation of the model

This subsection presents the static model in the non-stationary or transient state and the validation of measured and modelled results. Figure 6 shows the various examples of contour displays of temperature distribution on the rear of the PV module at different input parameters.

G = 46 W/m² G = 249 W/m² G = 579 W/m²
α = 6,1 W/m²°C α = 8,0 W/m²°C α = 13,7 W/m²°C
T_a = 3.5 °C T_a = 6.4 °C T_a = 8.0 °C
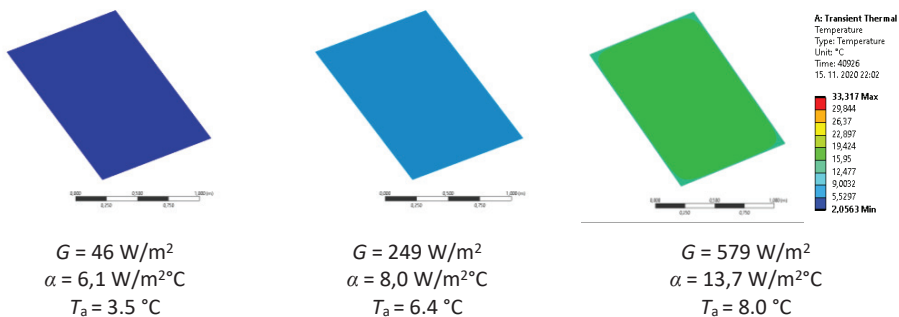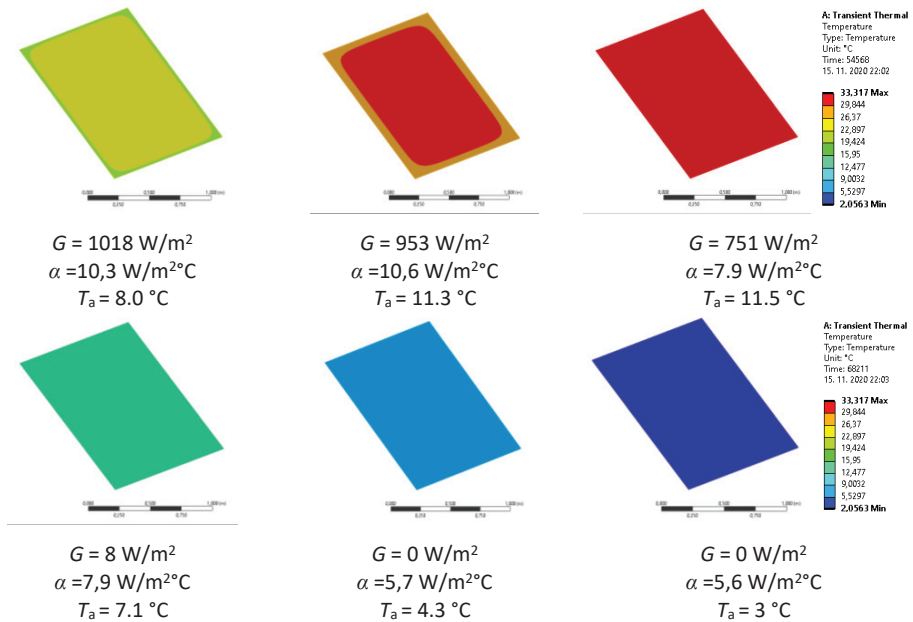
*Figure 6: Contour display of temperature distribution at different solar radiations G, thermal transmittance coefficients α and ambient temperatures T*a.

The three most essential parameters also presented as the boundary conditions of the static model are pre-arranged using the aforementioned equations (2.11-2.13). However, the boundary condition of heat flux (solar radiation) also considers the optical losses, which can be determined as a constant value, or as the function of the incidence angle of the Sun's rays. Figure 7 shows the validation between the measured and modelled values of the temperature distribution in the PV module for randomly selected days of the year (different weather conditions).
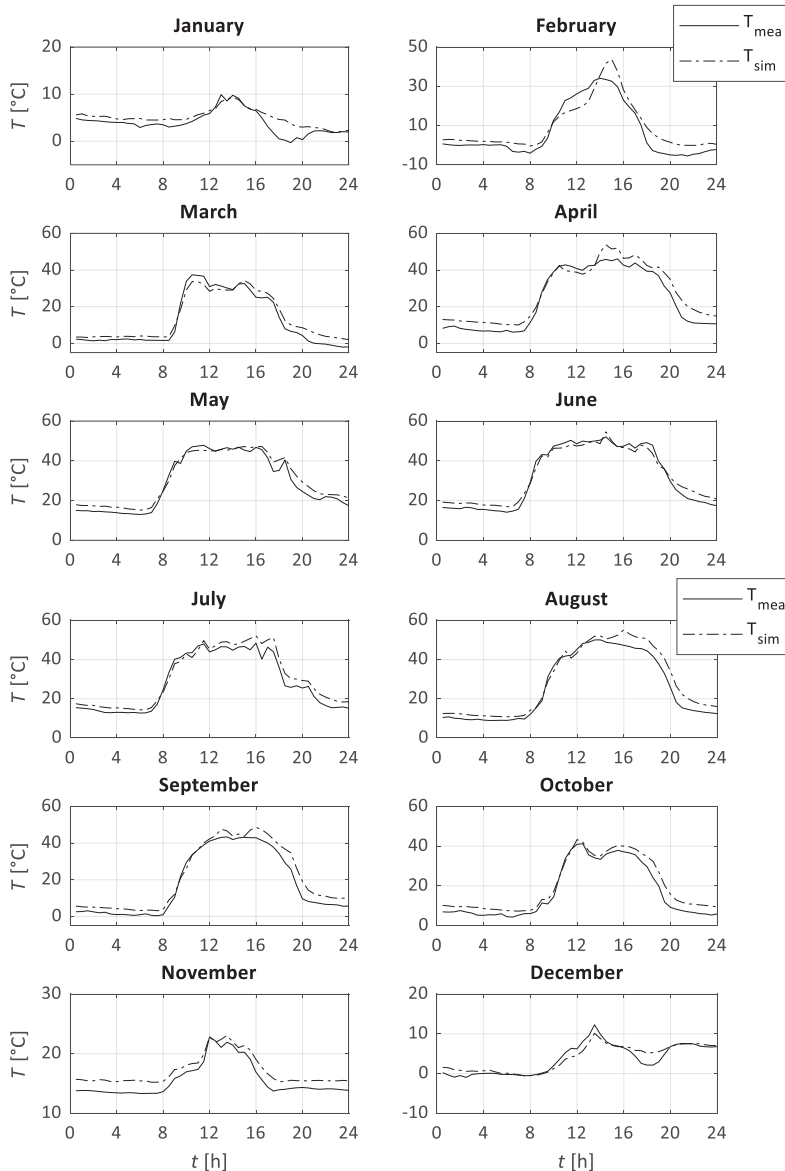
Figure 7: *Validation of the model with measurements (12 randomly selected days of the year).*

As mentioned above, the static model was performed in a non-stationary state due to easier comparison with the measurements. Figure 7 shows a slight deviation between temperatures in the summer months due to a smaller proportion of diffused solar radiation. However, the deviation in the parts without sunlight remains relatively high. In this part of the day, convection has a much more significant impact than radiation, which can be related to the measurement error of ambient temperature and wind speed.

A regression analysis was performed for a more comprehensive comparison between the measured and modelled values of the temperature distribution of the PV module. The assessment of the suitability of regression models is determined on the basis of the coefficient of determination R^2 (0 - mismatch, 1 - match).
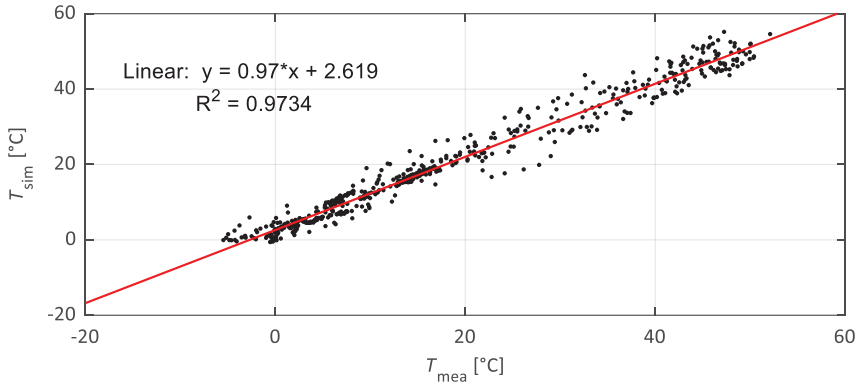
Figure 8: *Regression analysis between measured and modelled values of temperature of the PV module.*

The results in Figure 8 show a good concurrence between the measured and modelled values of the PV module temperature. It is also essential to highlight the consideration of the optical losses in the glass and PV cell layer (absorptivity, transmissivity, and reflectivity). In addition to optical losses, it is essential to consider the part of solar radiation that is converted into electricity. Since the measuring equipment does not include electrical quantities (DC voltage and DC current), it is almost impossible to determine the exact proportion of electricity.

4   CONCLUSION

This paper presents the static model of temperature distribution in a PV module performed in the Ansys Transient Thermal software package. The aim of the paper is to validate the static model of the PV module with measurements and presentation of the obtained results. The calculation of the temperature distribution in the PV module is based on measurements of solar radiation, ambient temperature, and wind speed. The static model was performed in a non-stationary state (as a function of time) and represents the change of input parameters in a half-hour time interval. The heat transfer calculation based on the static model was performed for 12 randomly selected days of the year. The results show a good concurrence between the measurements and the results of the static model. It can also be seen that more accurate results occur in the summer months due to a larger proportion of the direct solar radiation. A more significant deviation occurs in the winter months, where a higher proportion of diffuse solar radiation is present. In addition, it is essential to highlight that the regression analysis shows a larger deviation between the measurements and the results of the static model at higher temperatures and during the cooling time of the PV module.

References

[1]   **H. M. Ali:** *Recent advancements in PV cooling and efficiency enhancement integrating phase change materials-based systems – A comprehensive review*, Solar Energy, Vol.197, p.p. 163-198, 2020

[2]   **L. Brottier, R. Bennacer:** *Thermal performance analysis of 28 PVT solar domestic hot water installations in Western Europe*, Renewable Energy, Vol.160, p.p. 196-210, 2020

[3]   **B. Widyolar, L. Jiang, J. Brinkley, S. K. Hota, J. Ferry, G. Diaz, R. Winston:** *Experimental performance of an ultra-low-cost solar photovoltaic-thermal (PVT) collector using aluminum minichannels and nonimaging optics*, Applied Energy, Vol.268, p.p. 114,894, 2020

[4]   **S. Harjit:** *An Experimental comparison of two solar photovoltaic-thermal (PVT) energy conversion systems for production of heat and power*, Energy and Power, Vol.2, p.p. 46-50, 2012

[5]   **B. D. Perović, D. O. Klimenta, M. D. Jevtić, M. J. Milovanovića:** *Thermal Model for Open-Rack Mounted Photovoltaic Modules Based on empirical correlations for natural and forced convection*, Thermal science, Vol.23, p.p. 3,551-3,566, 2019

[6]   **C. Li, S. V. Spataru, K. Zhang, Y. Yang, H. Wei:** *A Multi-State Dynamic Thermal Model for Accurate Photovoltaic Cell Temperature Estimation*, IEEE Journal of Photovoltaics, Vol.10, No.5, p.p. 1,465-1,473, 2020

[7]   **J. Barry, D. Böttcher, K. Pfeilsticker, A. Herman-Czezuch, N. Kimiaie, S. Meilinger, C. Schirrmeister, H. Deneke, J. Witthuhn, F. Gödde:** *Dynamic model of photovoltaic module temperature as a function of atmospheric conditions*, Adv. Sci. Res., Vol.17, p.p. 165-173, 2020

[8]   **W.Z. Leow, Y.M. Irwan, M. Asri, M. Irwanto, A.R. Amelia, Z. Syafiqah, I. Safwati:** *Investigation of Solar Panel Performance Based on Different Wind Velocity Using ANSYS*, Indonesian Journal of Electrical Engineering and Computer Science, Vol.1, No.3, p.p. 456-463, 2016

[9]   **King, D.; Boyson, W.; Kratochvil, J.:** *Photovoltaic array performance model*, Tech. Rep. 2004, p .3,535

[10]   **Li, C.; Spataru, S.V.; Zhang, K.; Yang, Y.; Wei, H.:** *A Multi-State Dynamic Thermal Model for Accurate Photovoltaic Cell Temperature Estimation,* IEEE J. Photovolt., Vol.10, p.p. 1,465-1,473, 2020

[11]   **Barry, J.; Böttcher, D.; Pfeilsticker, K.; Herman-Czezuch, A.; Kimiaie, N.; Meilinger, S.; Schirrmeister, C.; Deneke, H.; Witthuhn, J.; Gödde, F.:** *Dynamic model of photovoltaic module temperature as a function of atmospheric conditions,* Adv. Sci. Res., Vol.17, p.p. 165-173, 2020

[12]   **Yu, Q.; Hu, M.; L.; J.; Wang, Y.; Pei, G.:** *Development of a 2D temperature-irradiance coupling model for performance characterizations of the flat-plate photovoltaic/thermal (PV/T) collector,* Ren. Ener., Vol. 153, p.p. 404-419, 2020

[13] **Sredenšek, K.; Štumberger, B.; Hadžiselimović, M.; Seme, S.; Deželak, K.:** *Experimental Validation of a Thermo-Electric Model of the Photovoltaic Module under Outdoor Conditions,* Appl. Sci., Vol.11, p. 5,287, 2021

[14] **Liu, B.Y.H., Jordan, R.C.:** *Daily insolation on surfaces tilted towards the equator,* ASHRAE JOURNAL, Vol.3, p.p. 53-59, 1961

[15] **Jimenez, J.I.:** *Effects of solar radiation on the performance of pyrometers with silicon domes*, J. Atmos. Ocean. Technol., Vol.5, p.p. 666-670, 1988

[16] Klucher, T.M.: *Evaluation of models to predict insolation on tilted surfaces,* Sol. Energy, Vol.23 (2), p.p. 111-114, 1979

[17] **B. Pentenrieder:** *Finite Element Solutions of Heat Conduction Problems in Complicated 3D Geometries Using the Multigrid Method*, Thesis, Technical University of Munich, Faculty of Mathematics, 2005

[18] **G. Gimenez, M. Errera, D. Baillis, Y. Smith, F. Pardo:** *Analysis of Dirichlet-Robin interface condition in transient conjugate heat transfer problems*, Application to a flat plate with convection 11th European Conference on Turbomachinery Fluid Dynamics and Thermodynamics - ETC 2015, MADRID, Spain, 2015

[19] **Photovoltaic modules - PVF 260.** Available online: http://www.pvfuture.eu/static/uploaded/pdf/PVF60M_SLO.pdf (accessed on 30 June 2021)

Nomenclature

(Symbols)	(Symbol meaning)
A	wall surface area
c_p	heat capacity
G_b	direct component (beam) of solar radiation
G_d	diffuse component of solar radiation
G_h	solar radiation on horizontal surface
G_t	solar radiation on tilted surface
i	Incident angle of the Sun's rays
L	length
n	vector
q	heat flux
q_s	heat flux from the body/domain
q_x	heat flux along x-axis
q_y	heat flux along y-axis
q_z	heat flux along z-axis

T		temperature
T_a		ambient temperature
T_f		fluid temperature
T_s		wall temperature
V		wind speed
V		volume
α		convective heat transfer coefficient
α_s		solar altitude angle
β		inclination angle
δ		boundary layer thickness
ε		emissivity of the body surface
λ		thermal conductivity
ρ		density
ρ_r		reflection factor
σ		Stefan-Boltzmann's constant
PV		photovoltaic
STC		standard test conditions
FEM		finite element method
EVA		ethylene-vinyl
PVF		polyvinyl fluoride